
Image-Guided Radiofrequency Ablation for Small Renal Masses

6

Emily F. Kelly and Raymond J. Leveillee

Abbreviations

CA	Cryoablation
EMN	Electromagnetic navigation
MWA	Microwave ablation
NSS	Nephron-sparing surgery
PN	Partial nephrectomy
RCC	Renal cell carcinoma
RFA	Radiofrequency ablation
RN	Radical nephrectomy
SRM	Small renal masses
TA	Thermal ablation

Key Messages

- As provider experience improves and long-term outcome studies become available, thermal ablation is becoming increasingly accepted as a potential new standard of care for solid small renal masses.
- Radiofrequency ablation (RFA) can be delivered using various percutaneous image-guided or laparoscopic techniques.
- The mechanism of action of RFA depends on the principle of heat conduction inducing cellular death.
- Emerging data show that long-term efficacy of radiofrequency ablation for managing small renal masses is approaching that of partial nephrectomy.
- Radiofrequency ablation offers fewer complications, faster convalescence, shorter hospital time and an option for patients who cannot undergo general anaesthesia.

E.F. Kelly, M.S. (✉) • R.J. Leveillee, M.D.,
F.R.C.S.-G.
Department of Urology, Florida Atlantic University,
Charles E. Schmidt College of Medicine, East
Bethesda Hospital, Boynton Beach, FL, USA
e-mail: rleveillee@bhpgdoc.com

6.1 Introduction

The diagnosis of incidental small renal masses (SRM), most commonly renal cell carcinoma (RCC), has increased during the past two decades due to the increased availability and utilization of

imaging [1, 2]. Since 1970, the incidence of RCC has increased 3 and 4% per year in the Caucasian and African-American populations, respectively. SRM encompass clinical stage cT1a <4 cm [3]. In recent years, the standard treatment of SRM has shifted from radical nephrectomy (RN) to nephron-sparing surgery (NSS) in which partial nephrectomy (PN) has become the new standard of care for tumours which do not invade the collecting system [4]. The goal of NSS is to resect/ablate the tumour and small surrounding rim of healthy tissue to ensure negative margins while preserving an optimal amount of renal function, i.e. “collateral damage” [4, 5]. While allowing for the preservation of normal renal parenchyma, NSS is associated with improved long-term outcomes. NSS options include PN, thermal ablation (TA) and nonthermal ablation (irreversible electroporation) where cryoablation (CA), microwave ablation (MWA) and radiofrequency ablation (RFA) are the most common forms of TA [5]. The decision between procedures is based on the experience of the team, urologist and interventional radiologist and access to equipment. It is beyond the scope of this review to discuss in detail these alternative options; thus, we will primarily focus on RFA.

6.2 Management Guidelines for RFA

Currently the literature suggests that RFA is most successful in SRM <4 cm. In 2009, the American Urological Association (AUA) published clinical guidelines for treatment of SRM. TA was suggested as a treatment option in patients with T1a tumours and major co-morbidities and/or patients unable to undergo surgery. This includes patients of increased age, renal insufficiency, bilateral tumours and local reoccurrence and patients with VHL syndrome. Additionally, the update suggested TA as an option in healthy patients with T1a/b lesions, as well as patients with major co-morbidities with stage T1b tumours [6, 7]. Furthermore, the European Association of Urology recommends TA not only for patients with major co-morbidities but for healthy patients

with SRM. Although PN remains the standard of care, this treatment modality is associated with increased warm ischemic time and increased risk of urologic complications including haemorrhage and urinary fistula formation. Compared to PN, TA offers fewer complications, faster convalescence, shorter hospital time and an option for patients who cannot undergo general anaesthesia.

6.3 Support/Results

Gervais et al. report a retrospective series of 100 renal tumours treated with RFA. One hundred percent of SRM <3 cm, 92% of 3–5 cm masses and 25% of masses >5 cm were treated successfully [1, 2]. Zagoria et al. demonstrate that with each 1 cm increase in diameter above 3.6 cm, the likelihood of recurrence-free survival decreases by a factor of 2.19 and recommends caution when treating tumours >4 cm [8]. Olweny et al. compare the 5-year outcomes for RFA vs. PN in T1a-treated RCC and report 97.2% vs. 100% ($p = 0.31$) cancer-specific survival, 97.2% vs. 100% ($p = 0.31$) overall survival and 91.7% vs. 94.6% ($p = 0.96$) local recurrence-free survival [9]. Psutka et al. report on 185 patients with T1 RCC followed for a mean of 6.43 years. The overall disease-free survival rate was 88.6% (92.3% T1a and 76.3% for T1b), and only 13% of patients were retreated for recurrence [10]. Please refer to Table 6.1 for additional results.

6.4 Principles of Radiofrequency Ablation

6.4.1 Mechanism of Action

RFA, a form of hyperthermal ablation, was originally developed for the treatment of aberrant cardiac pathways and now is used for renal masses and prostate hyperplasia. The main mechanism of RFA depends primarily on the principle of heat conduction inducing cellular death [4]. Secondary mechanisms include vaporization and coagulative necrosis. Alternating current with a

Table 6.1 Long-term outcomes following RFA for SRM

	Ma et al. [33]	Lorber et al. [13]	Kim et al. [34]	Zagoria et al. [8]	Tracy et al. [35]	Balageas et al. [36]	Ramirez et al. [37]
Pt number	52	50	47	41	208	62	79
Tumour number	58	53	48	48	243	71	111
Tumour size	2.2	2.3 (0.3–4.0)	2.3 (1.0–3.0)	2.6 (0.7–8.2)	2.4	2.3	2.2 (0.9–4.2)
Approach: lap percutaneous	24 34	24 29	12 36	0 48	68 172	0 71	111 0
Long-term F/U (months)	60.1 (48–90)	65.6 (48.5–120.2)	49.6	56 (36–64)	27 (1.5–90)	38.8 (18–78)	59 (2–120)
Incomplete ablation	0%	0%	10.4% (n = 5)	NA	2.9% (n = 7)	4.8% (n = 3)	2.5% (n = 2)
Local reoccurrence	5.1%	7.5%	8.3%	12% (n = 5), (0% <4 cm)	3.7% (n = 9)	12.7% (n = 9)	6.3% (n = 5)
Recurrence-free survival	94.2%	92.5	NA	88%	93%	NA	93.3%
Disease-free survival (5 years)	NA	90.6%	NA	83%	NA	61.9%	NA
Overall survival – 5 years/10 years	95.7% 91.1%	98% 93%	NA NA	66% NA	93% Na	82.3% 60.9%	72% NA
Cancer-specific survival	100%	100%	NA	NA	99%	96.8%	100%
Metastasis	0%	1.9%	0%	7% (n = 3)	1.2%	6.5%	0%
Probe type	14-G starburst XL	Cool-tip (90%) StarBurst RITA (10%)	Cool-tip	Cool-tip	StarBurst XL	LeVeen	Starburst XL

frequency between 375 and 900 KHz is delivered by a generator to an electrode probe which has been placed in the centre of the target tissue. Most often these systems are monopolar thus requiring a single grounding pad. The ablation zone of thermal conductivity remains unmodified 1–2 mm from the tip of the needle probe [11]. The resulting coagulation provides an advantage of RFA since no topical haemostatic agents are required post-ablation to control bleeding as has been seen with CA [4]. The effects of RFA-induced cellular injury rely on a time-temperature curve where ablations at higher temperatures require less time. Bhowmick et al. describe this phenomenon demonstrating that irreversible cellular damage occurs after 60 min at 45 °C, 5 min at 55 °C or 1 min at 70 °C [5]. As temperature increases, ionic agitation of intracellular mole-

cules develops resulting in frictional heating. Once temperatures reach above 60 °C, the cell loses its intracellular buffering capacity which results in the accumulation of intracellular calcium and eventual cellular death. As local inflammation increases, acidosis occurs and coagulative necrosis results [1, 2]. As the temperature increases, different phases of cellular damage are observed. Coagulation and cellular damage, secondary to protein denaturation, blood coagulation and irreversible cellular death, result after exposure to temperatures between 50 and 80 °C for seconds to minutes. Vaporization damage resulting in dehydration, vacuole formation and tissue ablation occurs at temperatures above 100 °C. Lastly, carbonization in the form of melting and charring transpires once temperatures reach between 150 and 300 °C [4]. Carbonization

is to be avoided as a zone of extremely high impedance results, thus limiting RF current passage and thermal spread.

The success of RFA depends on a temperature-based algorithm and treatment endpoints detected by temperature monitors, temperature probes and impedance probes [12]. We recommend that a temperature goal of at least 60 °C be obtained in order to achieve instantaneous irreversible cell damage by denaturation of proteins and coagulative necrosis (Fig. 6.1). General, conscious and intravenous sedation are anaesthetic options for RFA procedures; general anaesthesia is ideal. Under general anaesthesia, the respiratory cycle can be manipulated allowing for more accurate probe placement [1, 5].

6.4.2 Effect of Tumour Size and Location

Tumour size and location are strong predictors of ablative success [13, 14]. Heat loss is directly dependent on the average blood flow within a tissue. Therefore, when flow rates increase, “heat sinking” occurs and is responsible for the observed increased rate of incomplete ablations of vascular tumours, secondary to the location of proximal vessels [4, 5, 11]. Limitations of RFA are determination of end treatment, probe placement during different stages of the respiratory cycle and accu-

mulation of error which is seen between steps. End treatment goal is debated since heat cannot be visualized by CT or US. It has been demonstrated, however, that real-time temperature monitoring through non-conducting fibre optic probes allows for the establishment of adequate treatment endpoints and expands the size and location of tumours treated [4, 12, 13, 15, 16].

6.4.3 Advances: Real-Time Temperature Monitoring

Determination of the endpoint of treatment can be achieved with real-time temperature monitoring using fibre optic temperature probe(s) (Luxtron Corp., Santa Clara, CA). The use of these probes which are non-conductive allows for the determination of the precise temperature of the ablation zone in real time. Determination of end treatment when all probes reach at least 60 °C at the tumour periphery decreases the number of incomplete ablations and improves precision [5, 12, 13, 16].

6.4.4 Not All RF Probes Are the Same

The mechanism of action whereby RF generates temperatures is via metal electrode/tissue interactions. Alternating electromagnetic (AC) waves (between 10 kHz and 900 MHz) pass through tissues and result in ionic agitation with subsequent heat generation. At the probe/tissue interface, a significantly high proportion of current density occurs creating potentially extremely high local temperatures with resulting carbonization which ultimately inhibits heat conduction. The goal is to heat at lower sustained temperatures and not cause carbonization (avoid “charcoaling”). Several engineering designs have been employed to try to obviate this high current density – these include expanding the surface area with deployable needles, LeVein® RF system 3000® (Boston Scientific, Natick, MA, USA) and RITA StarBurst® (Angiodynamic®, Queensbury, NY, USA), as well as internal cooling to prevent tissue desiccation at the metal/tissue contact point,



Fig. 6.1 Gross image (confirmed histologically) demonstrating complete destruction of 4.7 cm left renal clear cell carcinoma via coagulative necrosis. The kidney removed at 12 months follow-up after being treated successfully by laparoscopic RFA, Cool-tip® (Valley Lab, Boulder, CO, USA) under laparoscopic US image guidance

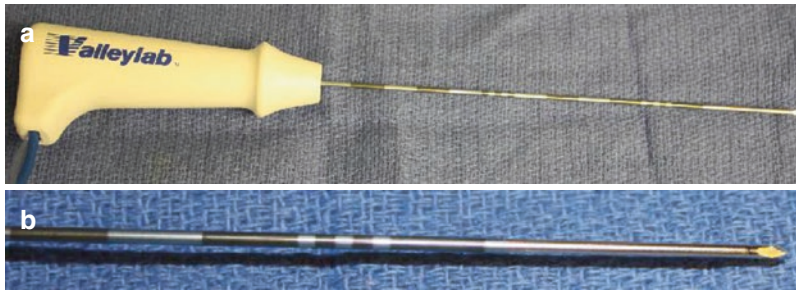


Fig. 6.2 (a) The straight needle, Cool-tip® (Covidien, Valley Lab, Boulder, CO, USA) probe with hand piece. Circulation of chilled water into the hollow channel of the needle prevents overheating and charring allowing for

wider dissemination of electrical current. (b) Close up of Cool-tip® demonstrating uninsulated active tip (*bracket*) and centimetre calibrations proximally

Fig. 6.3 The multilined, expandable RITA StarBurst® (Angiodynamic®, Queensbury, NY, NY, USA) electrode. Adjustable tine spacing allows for single needle placement creating a predictable expansion of the tines. Extreme expansion may create nonspherical lesions due to conductive heat loss



Cool-tip® (Covidien, Boulder, CO, USA). This allows electrical current to emanate away from the metal antenna and still create heat several mm away from the needle probe. Saline tissue perfusion (Talon™, Angiodynamic®, Queensbury, NY, USA) will spread current density away from the metal tip and increase the ablation target zone (Figs. 6.2 and 6.3) [2, 5]. It is beyond the scope of this manuscript to describe in great detail the pros and cons of each design; however, we feel it is important for the reader to be cognizant of the fact that not all RFA probes work the same. This may impact interpretation of results seen in Table 6.1.

6.4.5 Contraindications

RFA is contraindicated in patients who have a life expectancy of less than 1 year, multiple sites of metastasis at the time of procedure, the presence

of an irreversible haematological coagulopathy and/or result of respiratory complications when in the prone or supine position for the length of the procedure.

6.5 Percutaneous Radiofrequency Ablation

Percutaneous RFA is utilized for most tumours but is optimally suited for laterally and posteriorly located renal masses away from vital intraperitoneal organs. In contrast, the laparoscopic approach allows for the manipulation of the surrounding anatomy in anteriorly located tumours, limiting thermal damage [4]. Imaging is often utilized for laparoscopic RFA; however, presently this is limited to ultrasound for probe placement. We will focus our discussion on percutaneous needle placement; imaging techniques include conventional

computerized tomography (CT); CT fluoroscopy; magnetic resonance imaging (MRI), possibly augmented by three-dimensional renderings; and image fusion techniques [1, 4]. Of these techniques, CT-guided RFA is most commonly utilized [5, 17].

6.5.1 CT-RFA

CT-RFA can be achieved in either the prone or lateral decubitus position allowing for access to posteriorly or laterally located tumours. The authors recommend that CT-RFA be performed under general anaesthesia allowing for accurate probe placement under the guidance of a CT grid [1, 4, 11]. This prevents patient movement and helps regulate the breathing cycle – thus improving accuracy. After the initial skin incision is made, a 16 gauge biopsy cannula is guided by means of intermittent CT imaging. Once the position is confirmed, the stylet is withdrawn. Next, via the cannula, fine needle aspiration can be performed (optional) with a 22 gauge Chiba needle. Alternatively (authors' preference) core needle biopsies are obtained, through an 18 gauge spring-loaded biopsy needle [1, 4]. A minimum of three cores are encouraged. At this time, the TA probe is placed in the same trajectory as the biopsy needle but *not* through the metal biopsy guide as this will increase the risk of capacitive currents and collateral damage, especially skin burns. Once the TA probe is radiographically

confirmed to be in proper position, ablation is performed according to manufacturer's specifications and clinician's judgement (Fig. 6.4). Ablation of the access tract is recommended to ensure cellular death and to aid in haemostasis. Post-ablation the probe is withdrawn and a small adhesive bandage is applied. Local anaesthetic (lidocaine 1% or Marcaine 0.25%) can be utilized at the puncture site but is optional. It is reasonable to perform an end of procedure CT image to document any perirenal fluid collections such as haematoma or urinoma. If intercostal access is utilized, a post-procedural chest radiograph is recommended to rule out thoracic complications such as pneumothorax or haemothorax. Follow-up imaging is performed typically at 6 weeks, 6 months and annually for up to 5 years [1, 4, 11, 32].

CT-RFA has several advantages in comparison to the laparoscopic approach. First, access to CT scanners is ubiquitous [17]. Next, the length of hospital stay is decreased, since patients can receive ablation at outpatient facilities which further decreases the cost of the procedure. Furthermore, complications of insufflation and laparoscopic manipulation of vital organs are avoided resulting in fewer post-procedural complications [4]. Limitations of this approach include diameter of gantry opening, patient size, time required for needle repositioning, patient exposure to radiation and contrast material and inability of real-time monitoring [11, 17].

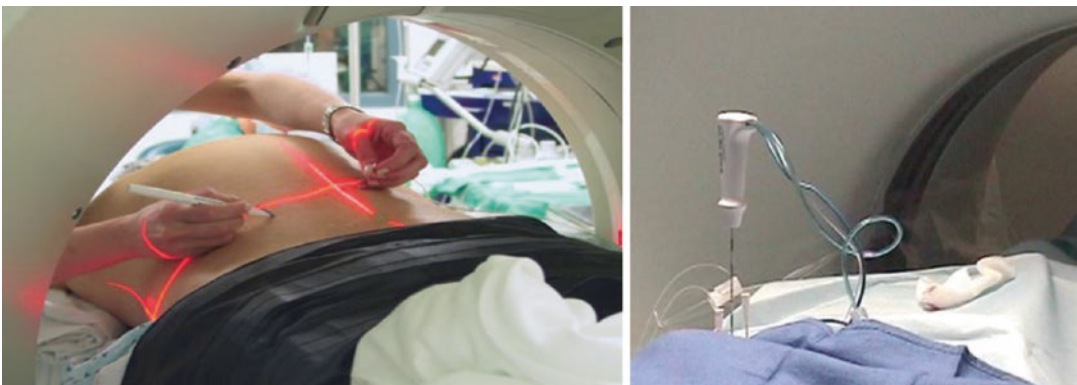


Fig. 6.4 (a) Patient, under general anaesthesia, placed on standard CT gantry. Laser cross-hairs projected to guide fingertip control of needle placement. (b) Post hand-assisted RFA probe placement

6.5.2 MRI-RFA

Although MRI-compatible RFA machines are not standard in interventional radiology suites, MRI-guided RFA provides several advantages when compared to CT-guided techniques. MRI-RFA was first described by Anzai et al. in 1995 for the treatment of brain tumours. Later Gervais and Mayo-Smith et al. have reported successful MRI-RFA for renal tumours. RFA is best performed with open-magnet MRI machines, for which two systems are available. The low-field biplanar scanner provides room for the provider to access the patient for probe employment. The high-field short-bore magnet design affords high temporal and spatial resolution however does not afford the physician as much room to access the patient for probe placement [2]. In order for RFA to be utilized under MRI guidance, MRI-compatible equipment is obligatory [4]. Two electrodes have been specifically developed for MR use. First, the nitinol StarBurst Semi-Flex® (Angiodynamic®, Queensbury, NY, NY, USA) electrode provides a more malleable shaft for triangulation and a larger ablation zone through the use of several dynamic tines [2]. The second, the titanium Cool-tip RF system® (Covidien, Boulder, CO, USA), provides maximum ablation size while simultaneously cooling with circulating water [2, 4]. Lewin et al. describe effective MRI-RFA treatment delivered through the Cool-tip RF system® for 12–15 min at 90 °C guided via real-time temperature probes [4].

Axial-fast spin-echo imaging allows for the planning of probe entry. The trajectory is then placed under continued MR guidance. Guidance can be aided by either the three-slice method or the triorthogonal image plane method. While centred on the probe shaft, the three-slice method utilizes three parallel 5 mm slices providing feedback of deviance from the focus of the middle slice of the preset trajectory allowing the provider to advance along the correct path. The triorthogonal image plane uses modifiable sagittal, coronal and axial scans which are taken in real time to form a single image which is then projected on the patient to guide the path of the probe along the trajectory [2]. Both the three-slice and

triorthogonal image plane methods are tools to help improve probe placement accuracy.

High spatial resolution images allow for target confirmation. If the StarBurst Semi-Flex® electrode is utilized, an additional step must be completed to assure that the tines are evenly deployed and are at the level of the target and that the target has remained in the original position. Confirmation of tine placement is achieved via multiplanar imaging [2].

Ablation is then monitored via short tau inversion recovery (STIR) T2-weighted images. Successful ablations appear hypointense while enhanced lesions require repeat ablation. Once successful ablation is confirmed and probes are removed, post-ablation T1-weighted series are obtained to further ratify total tumour ablation, again by the absence of image enhancement [2]. Boss et al. reported that the repositioning of electrodes in tumours larger than 3.0 cm may be required to achieve complete ablation. Gervais et al. achieved successful MRI ablation in tumours as large as 5 cm [18]. Advantages of MRI-RFA include non-invasive real-time temperature assessment and elimination of ionizing radiation. Disadvantages of MRI-RFA include lengthier procedure time, incompatibility of ECG machines to monitor high-risk cardiac patients during the procedure, limited workspace of gantry, higher cost of machine and more limited availability, in comparison to CT. MRI-compatible RFA machines, unlike CT, may not be standard in all interventional radiology departments [1, 17].

6.5.3 Cone-Beam CT

Cone-beam CT-RFA uses a series of three-dimensional cross-sectional images to help guide the clinician along the predetermined trajectory path. Systems available include DynaCT (Artis Zeego, Siemens Medical Solutions, Erlangen, Germany), Innovact (GE Healthcare, Schenectady, NY) and XperCT (Phillips Healthcare, Amsterdam, Netherlands). Digital fluoroscopy coupled with these systems helps create a 3D reconstruction of the target tissue. Via the rotation

Fig. 6.5 Cone-beam CT room set-up. Notice the increased work space for probe placement. Screen highlights monitor used for fluoroscopic image guidance of needle placement (*yellow circles*)



of the large C-arm, hundreds of images from different angles can be taken via rotational fluoroscopy (Fig. 6.5). These images can then be manipulated at the work station to create CT quality images. Additional software allows triplanar trajectory planning for probe/needle placement under fluoroscopic guidance. The entry point is then projected onto the patient via a cross-hair laser beam to guide the initial trajectory. Further needle manipulation is enhanced by preset fluoroscopic targeting paths (Fig. 6.6) [1]. Preliminary studies have shown comparable outcomes with shorter procedure times and decreased radiation exposure for patient and staff [19, 20].

Advantages of using this modality are increased work space for probe placement, increased biopsy and probe placement accuracy and decreased radiation exposure to the patient.

6.5.4 Electromagnetic Navigation

Electromagnetic navigation (EMN) combines and fuses pre-ablation CT scans with the EMN field to guide placement of the probe towards the target tissue in real time. The EMN field generator produces an alternate electromagnetic field which utilizes positioned voltage producing RFA sensors located within small coils of the needle [1, 11, 21, 22]. The information from the sensors is then combined with passive fiducial markers placed on the patient's peripheral skin allowing for the real-time fusion of pre-ablation CT with

the EMN system [1]. Systems which can be used include the Veran IG4 Plug-n-Play Delivery System (Veran Medical, St. Louis, Mo, USA) (Fig. 6.7) and the Aurora system (NDI, Waterloo, Ontario, Canada) [11]. Advantages of EMN include increased accuracy and decreased procedure time. However, the implication of this procedure can be expensive in obtaining the necessary hardware, coils and instruments [1].

6.5.5 Ultrasound CT Fusion

There are several different ultrasound CT fusion-based systems. Similar to the EMN system described above, US can be used in real time with the EMN system allowing for the fusion of pre-ablation CT, PET or US images. As in EMN, this system measures the voltage from the RFA needle coils; however, this information is then combined with in-procedure US to calculate needle position and angle selections for probe placement [1, 11, 21]. One system combining CT/PET images obtained pre-ablation with intraprocedural US was described by Venkatesan et al. using the PercuNav (Philips, Eindhoven, Netherlands). In combination with the already described EMN procedure, this system allows for PET/CT images to be fused on real-time US to guide the EMN tracked needle probes on the correct trajectory path towards the predetermined target. Post-confirmatory CT scans of needle probe placement showed a tracking error of

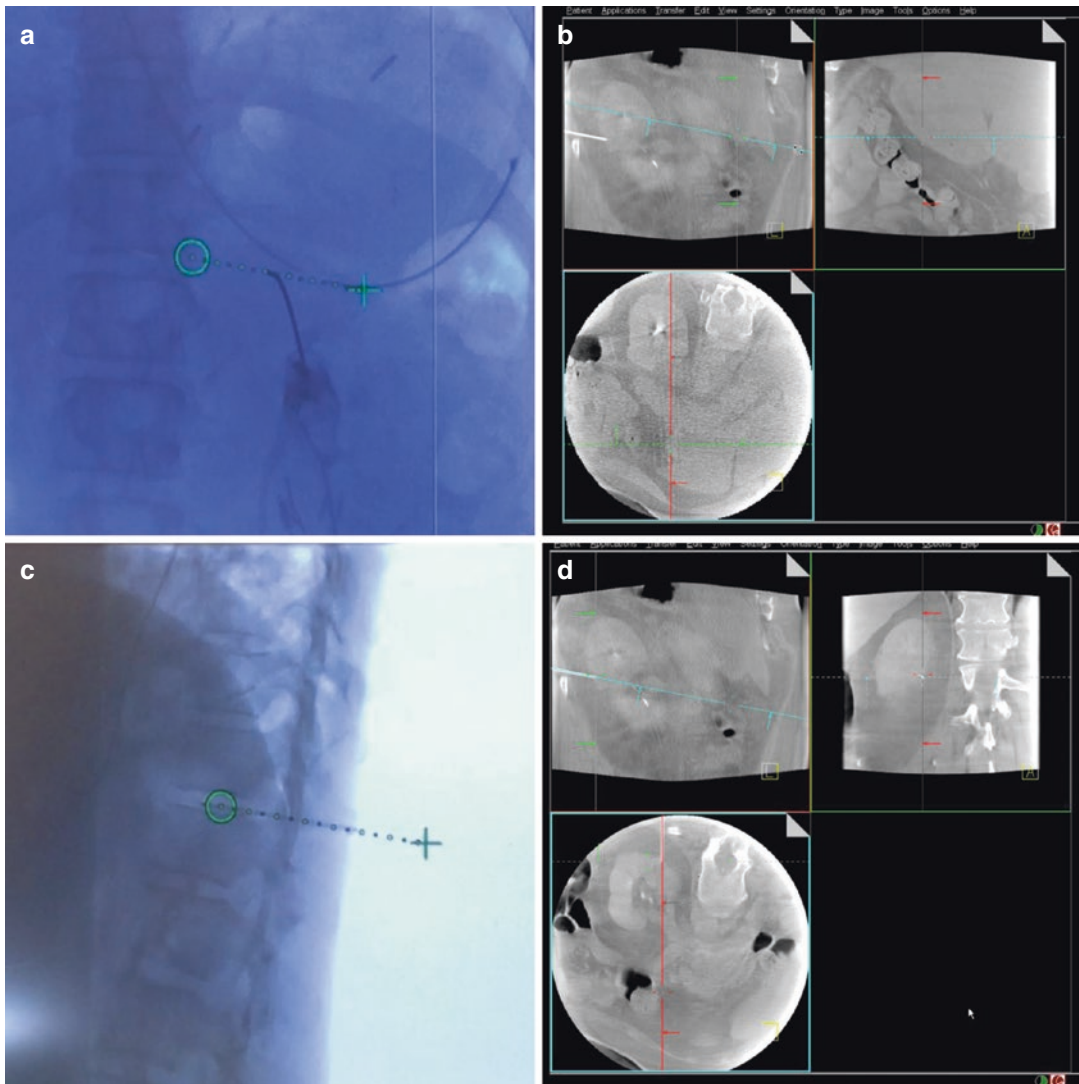


Fig. 6.6 Artis Q Zeego, Siemens, Germany, is utilized for probe placement. Movement of the C-arm aids in repositioning of the probe done under fluoroscopy. (a) Prior to fluoroscopic realignment, the trajectory, dotted line, is not aligned with the probe (yellow arrow) and placed in the

kidney. (b) Axial, coronal and sagittal projections of target lesion. (c) iGuide software (Siemens) planning allows for needle advancement with fluoroscopic targeting. Once the final position is attained, it is confirmed with an additional “spin” (d) before biopsy and TA treatment

5.85 ± 4.48 mm without adding increased procedural time [1, 23]. Krucher et al. described a similar system using EMN position tracking sensor (Traxtal Inc., Toronto, Canada), renamed Traxtal PercuNav (Philips Healthcare, Andover, MD, USA) (Fig. 6.8), attached to the probe handle in 40 patients undergoing renal and liver ablations. The average tip to target error of all ablations was 3.8 ± 2.3 mm; liver-specific target error of

4.0 ± 1.9 and renal target error of 3.4 ± 2.1 were demonstrated [21].

Hung et al. reported another US/CT or US/MR fusion system used for the ablation of 32 virtual tumours in 16 canine kidneys. This system utilizes the Global Positioning System (MyLab 70 XVG, Biosound Esaote) which combines a virtual navigation system with 2D US. Advantages include the ability of US-obtained real-time two-

dimensional images to be superimposed onto pre-procedural-obtained CT or MR images. This permits real-time navigation of probe position. In this study, the average tip to target error was 1.8 mm. The virtual navigator aspect of the system predicts the amount of tissue ablated during the procedure allowing the provider to calculate the amount of remaining target tissue still requiring ablation. This reduces the need for subsequent ablation sessions. The accuracy of the procedural calculated ablation percentage was

able to be determined after the animals were euthanized and gross specimen measurements were obtained. The performance results of the system were found to be significant ($r = 0.5$; $P = 0.006$) [24].

An advantage to the incorporation of US is real-time monitoring without exposure to radiation or contrast. However, there are many limitations. The quality of the image can become obstructed by bowel gas, RFA produced vaporization bubbles and large quantities of abdominal fat [25, 26].



Fig. 6.7 Veran IG4 Plug-n-Play Delivery System (Veran Medical, St. Louis, Mo, USA) and EMN system

6.5.6 Camera Feedback

A camera-based system has been developed which can be used with inoperative CT to create a real-time three-dimensional CT image. Through the use of two calibrated cameras, the patient’s respiration and movement can be tracked in real time allowing for precise placement of RFA probes. Target error has been reported as 2 mm in phantom and <5 mm in actual patients.

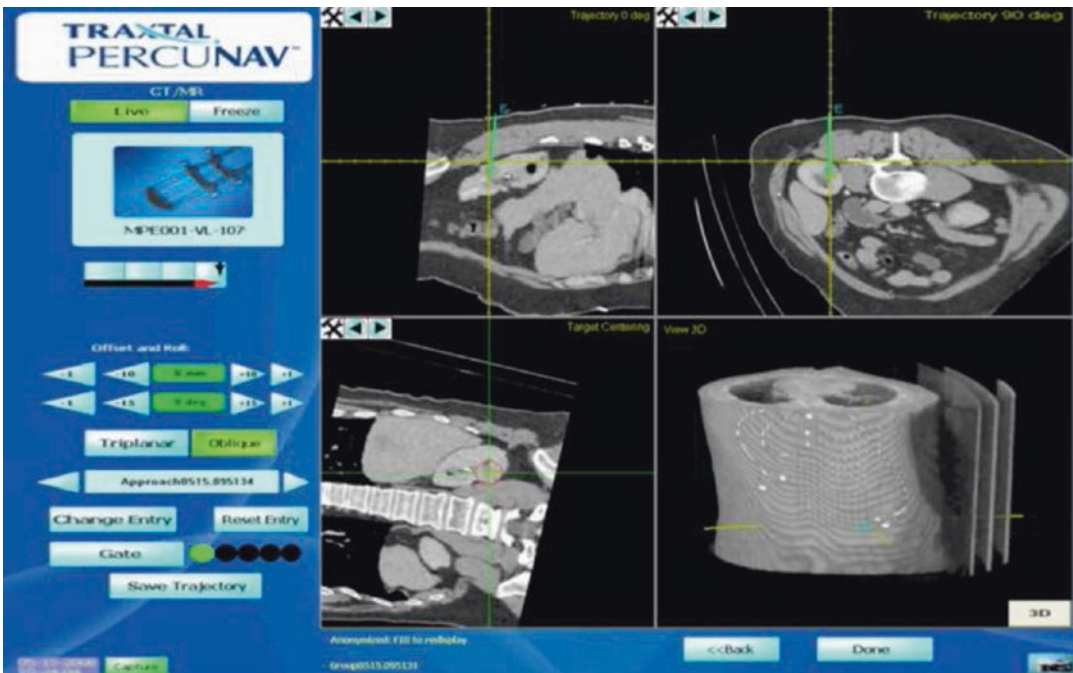


Fig. 6.8 Traxtal PercuNav (Philips Healthcare, Andover, MD, USA) ultrasound CT fusion-based system

6.5.7 Robot-Guided Ablation

This technique utilizes the CT-integrated robot (National Institutes of Health, Bethesda, MD, and Philips Medical Systems, Cleveland, OH) where the needle is placed mechanically along the trajectory [22].

Hong et al. further combined US/CT with a robotic needle holder. In this system, the alignment of the needle holder is robotically controlled allowing for compensation of respiration movement. The tip to target error reported in this system was 1.7 mm [1, 27]. Furthermore, with the use of a robot, radiation exposure to the urologist is eliminated when CT fluoroscopy is used. Other advantages of robotic needle placement include enhanced precision, accuracy and steadiness, when compared to human placement (Fig. 6.9). One challenge presented is in the mechanism of robotic movement which produces friction disrupting the insulation sheath of the probe. Solomon et al. are currently researching ways to improve this limitation. Other disadvantages include availability and increased set-up time [28].

6.5.8 Laser-Guided Ablation

This technology uses heat created by 700–1200 nm wavelength laser beam to achieve tumour ablation. CT, MRI or US can be used to direct the laser to the target tissue. A study conducted by Jacobi et al. utilized a laser-guided puncture support system (Partner-Diagnostica, Markt-Indersdorf, Germany). The advantage of this particular system

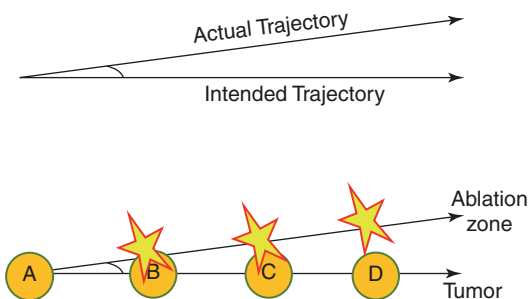


Fig. 6.9 Success in image-guided TA relies on precision. Even a misdirection of 1 or 2° can significantly impact targeting and efficacy

is that it can be mounted on all “standard” CT machines. The use of the laser showed a deviation between 1.7 and 2.3 mm compared to 2.0 and 4.0 mm without the aid of the laser over the course of 160 punctures ($P < 0.5$). The improved accuracy was especially noted in inexperienced users. However, due to the lack of long-term studies, this modality has limited clinical use [5, 29].

6.6 Laparoscopic RFA

Laparoscopic RFA is traditionally performed under US guidance for anterior tumours located within 2 cm of the bowel. The US image quality is limited by patient size, and the technique is difficult to master. Furthermore, US-guided needle placement is not as precise as CT-guided probe placement. Recently, laparoscopic DynaCT has been performed by Nozaki et al. for laparoscopic radical nephrectomy. This technique allows for the advanced ability to dissect and visualize the renal hilum while providing 3D planning allowing the surgeon to overcome limitations of conventional CT planning. This provides better operating room predictability and helps prevent unexpected surgical complications.

The authors of this chapter have recently performed the first known RFA ablation using laparoscopic thermal ablation (TA), in a hybrid operating room, using a fixed angiographic system (syngo DynaCT, Artis Q Zeego system, Siemens Healthcare GmbH, Forchheim, Germany). Patients who are not ideal candidates for partial nephrectomy are often offered with percutaneous CT-guided TA, as described above. In special circumstances, the tumour may be located too close to vital structures whereby collateral damage may occur. One option in these situations is instillation of isosmotic fluid to displace bowel (hydrodissection). Alternatively, laparoscopic exposure and simultaneous 3D imaging may be performed. The laparoscopic protocol is ideal for patients with anterior tumours located within 2 cm of the surrounding vital tissue (excluding the liver). This allows for the manipulation of vital structures while decreasing thermal injury to the spleen, bowel, ureter and other vital organs while further

reducing the number of post-procedural complications secondary to thermal injury. Coupling laparoscopic exposure with the DynaCT technology provides the advantage of enhanced precision of needle placement and decreased radiation exposure to the patient and staff as compared to conventional methods of targeting while avoiding damage to surrounding structures.

6.7 Complications of RFA

As with any invasive procedure, complications can occur and are usually decreased as technology improves and user experience increases. In general, TA offers significant safety as compared to other forms of NSS. Sterrett et al. described the results of a multi-institutional review for the long-term treatment outcomes of CA and RFA treatment of SRM compared to PN. The complication rate for PN was 13.7% compared to 8.3% for RFA [4]. Bleeding or post-ablation haemorrhage is the most common major complication observed in TA procedures. RFA which is haemostatic is associated with very infrequent bleeding complications. Haemorrhage is seen much more frequently as a complication of CA procedures when compared to RFA, especially for tumours >3 cm [30]. Ureteral or renal pelvic injury may also occur. TA if extended outside of the target tissue into the collecting system can result in urine leakage. Furthermore, ureteral injury secondary to stricture can result in hydronephrosis. Other complications include bowel injury, pneumothorax, tract seeding (risk <0.01%) and genitofemoral nerve injury, although less common. Injection of saline or 5% dextrose solution to displace the bowel is utilized by some interventional radiologists in order to increase spacing, thus limiting thermal injury. Unfortunately, this is not always successful technically [31].

6.8 Post-procedural Follow-Up

Success is defined by local recurrence and enhancement on imaging follow-up done by either MRI or CT imaging [5]. MRI serial images avoid the compounded effects of ionizing radiation over the post-ablation surveillance period.

The ablation zone appears hypointense on T2-weighted and STIR images and hyperintense on T1-weighted images [2]. Follow-up by CT scan does subject the patient to ionizing radiation, and success is guided by <20 HU enhancement and no evidence of growth in the ablation zone [4]. Currently there is controversy in the literature about how often post-ablation surveillance should be conducted. Most investigators recommend follow-up images be performed 3, 6 and 12 months' post-ablation then yearly thereafter for up to 5 years [25]. The AUA Guidelines on imaging after NSS, specifically post PN, call for imaging annually for a minimum of 3 years, for low risk, and 5 years, for high risk [32].

6.9 Long-Term Follow-Up

Several studies have matured to demonstrate long-term efficacy very comparable to that of PN for SRM. Recently, Olweny et al. showed that the 5-year oncologic outcomes of RFA vs. PN in T1a-treated patients with RCC were similar, both having a cancer-specific survival rate greater than 95% [9]. However, PN still remains the standard of care secondary to the lack of studies demonstrating long-term outcomes of TA. With the improvement of provider experience and the increased availability of long-term outcome studies, TA is becoming more widely accepted as a potential alternative for the treatment of solid SRM.

6.10 Other Ablative Techniques

6.10.1 Cryotherapy

CA, a form of hypothermic TA, induces cellular death via the freeze-thaw cycle using the Joule-Thomson principle. Cellular freezing is achieved via probe-delivered pressurized argon gas resulting in cellular dehydration and membrane rupture when temperatures reach between -30 and -40 °C. Tissue damage results in the formation of an ice ball which can be visualized by ultrasound guidance. Subsequent reperfusion injury occurs in the thawing stage, induced by helium, causing microcirculatory failure and small vessel thrombosis.

6.10.2 Microwave Ablation

MWA achieves cellular death through frictional heating produced by electromagnetic waves. A wavelength frequency between 300 MHz and 300 GHz is required to generate tissue necrosis via the high-speed movement of water molecules within the ablation zone. The rotation of water molecules results in the absorption of heat leading to cellular death and ablation. An advantage of MWA is the ability to achieve successful ablations in tissues with previous thermal damage, low thermal conductivity and/or high impedance. A disadvantage of MWA is that the technique produces a larger ablation zone compared to RFA, thus limiting its clinical use in anteriorly located tumours.

6.10.3 Irreversible Electroporation

IRE, a nonthermal ablative technique, causes cellular death and apoptosis via a contained electrical force field produced between percutaneously placed probes. The high-voltage electrical current produced increases the permeability of the cell membrane, disrupts the electrochemical gradient and results in apoptosis. The end result of apoptosis is achieved when the amperage and voltage of 20–50 A and 1500–3000 V are attained. The main advantage of IRE is that apoptosis is not the product of thermal damage or coagulative necrosis. As a result, this tissue-sparing modality can be utilized for masses in close proximity to vital organs. Additionally, IRE allows for the ability to delineate the ablation zone while avoiding the heat-sink phenomenon. Since IRE is rarely performed for renal masses, there is limited data on its long-term effectiveness and follow-up.

Conclusion

Although PN is currently the standard of care for the management of SRM, image-guided TA through laparoscopic and percutaneous approaches is gaining support as technology expands and long-term studies are conducted. TA, in our opinion, is the future gold standard of SRM treatment protocols. Improvements in

imaging modalities with ease of targeting to improve accuracy are being developed and perfected. With increased access, training and automation, TA will become a common practice. As more hospitals begin to integrate advanced imaging into “HYBRID” operating rooms, it is felt that possibly more surgeons will be performing these procedures as they broaden their armamentarium.

References

1. Glamore M, Leveillee R. CT-guided renal ablation. In: Liao JC, Su L, editors. *Advances in image-guided urologic surgery*. New York: Springer; 2015. p. 175–84. doi:10.1007/978-1-4939-1450-0.
2. Ordon M, Findeiss L, Landman J. MR-guided renal ablation. In: Liao JC, Su L, editors. *Advances in image-guided urologic surgery*. New York: Springer; 2015. p. 185–99. doi:10.1007/978-1-4939-1450-0.
3. Campbell SC, Novick AC, Beldegrun A, et al. Guideline for management of the clinical T1 renal mass. *J Urol*. 2009;182(4):1271–9.
4. Sterrett SP, Nakada SY, Wingo MS, Williams SK, Leveillee RJ. Renal thermal ablative therapy. *Urol Clin North Am*. 2008;35(3):397–414.
5. Castro A Jr, Jenkins LC, Salas N, Lorber G, Leveillee RJ. Ablative therapies for small renal tumours. *Nat Rev Urol*. 2013;10(5):284–91.
6. Castle SM, Gorbatiy V, Avallone MA, Eldefrawy A, Caulton DE, Leveillee RJ. Cost comparison of nephron-sparing treatments for cT1a renal masses. *Urol Oncol*. 2013;31(7):1327–32.
7. Gorin MA, Gahan J, Antebi E, Carey RI, Bird VG. Laparoscopic-guided radiofrequency ablation is safe for the treatment of enhancing renal masses among patients prescribed antithrombotic agents. *Clin Appl Thromb Hemost*. 2012;18(1):35–9.
8. Zagoria RJ, Pettus JA, Rogers M, Werle DM, Childs D, Leyendecker JR. Long-term outcomes after percutaneous radiofrequency ablation for renal cell carcinoma. *Urology*. 2011;77(6):1393–7.
9. Olweny EO, Park SK, Tan YK, Best SL, Trimmer C, Cadeddu JA. Radiofrequency ablation versus partial nephrectomy in patients with solitary clinical T1a renal cell carcinoma: comparable oncologic outcomes at a minimum of 5 years of follow-up. *Eur Urol*. 2012;61(6):1156–61.
10. Psutka SP, Feldman AS, McDougall WS, et al. Long-term oncologic outcomes after radiofrequency ablation for T1 renal cell carcinoma. *Eur Urol*. 2013;63(3):486–92.
11. Salas N, Castle SM, Leveillee RJ. Radiofrequency ablation for treatment of renal tumours: technological principles and outcomes. *Expert Rev Med Devices*. 2011;8(6):695–707.

12. Wingo MS, Leveillee RJ. Central and deep renal tumours can be effectively ablated: radiofrequency ablation outcomes with fibre optic peripheral temperature monitoring. *J Endourol.* 2008;22(6):1261–7.
13. Lorber G, Glamore M, Doshi M, Jorda M, Morillo-Burgos G, Leveillee RJ. Long-term oncologic outcomes following radiofrequency ablation with real-time temperature monitoring for T1a renal cell cancer. *Urol Oncol.* 2014;32(7):1017–23.
14. Ferakis N, Bouropoulos C, Granitsas T, Mylona S, Poulias I. Long-term results after computed-tomography-guided percutaneous radiofrequency ablation for small renal tumours. *J Endourol.* 2010;24(12):1909–13.
15. Carey RI, Leveillee RJ. First prize: direct real-time temperature monitoring for laparoscopic and CT-guided radiofrequency ablation of renal tumours between 3 and 5 cm. *J Endourol.* 2007;21(8):807–13.
16. Lay AH, Faddegon S, Olweny EO, et al. Oncologic efficacy of radio frequency ablation for small renal masses: clear cell vs papillary subtype. *J Urol.* 2015;194(3):653–7.
17. Uppot RN, Silverman SG, Zagoria RJ, Tuncali K, Childs DD, Gervais DA. Imaging-guided percutaneous ablation of renal cell carcinoma: a primer of how we do it. *AJR Am J Roentgenol.* 2009;192(6):1558–70.
18. Fallone BG, Moran PR, Podgorsak EB. Noninvasive thermometry with a clinical x-ray CT scanner. *Med Phys.* 1982;9:715–21.
19. Cheng EY, Naranje SM, Ritenour ER. Radiation dosimetry of intraoperative cone-beam compared with conventional CT for radiofrequency ablation of osteoid osteoma. *J Bone Joint Surg Am.* 2014;96(9):735–42.
20. Leveillee RJ, Castle SM, Salas N, Doshi M, Gorbatiy V, O'Neill W. Improved targeting of radio-frequency ablation probes and thermal sensors: a preliminary investigation of flat-panel CT guided ablation of renal tumours in the cardiac catheterization lab. *J Endourol.* 2011;25(7):1119–23.
21. Krucker J, Xu S, Venkatesan A, et al. Clinical utility of real-time fusion guidance for biopsy and ablation. *J Vasc Interv Radiol.* 2011;22(4):515–24.
22. Leveillee RJ, Ramanathan R. Optimization of image-guided targeting in renal focal therapy. *J Endourol.* 2010;24(5):729–44.
23. Venkatesan AM, Kadoury S, Abi-Jaoudeh N, et al. Real-time FDG PET guidance during biopsies and radiofrequency ablation using multimodality fusion with electromagnetic navigation. *Radiology.* 2011;260(3):848–56.
24. Hung AJ, Ma Y, Zehnder P, Nakamoto M, Gill IS, Ukimura O. Percutaneous radiofrequency ablation of virtual tumours in canine kidney using global positioning system-like technology. *BJU Int.* 2012;109(9):1398–403.
25. Venkatesan AM, Wood BJ, Gervais DA. Percutaneous ablation in the kidney. *Radiology.* 2011;261(2):375–91.
26. Boss A, Clasen S, Kuczyk M, Schick F, Pereira PL. Image-guided radiofrequency ablation of renal cell carcinoma. *Eur Radiol.* 2007;17(3):725–33.
27. Hong J, Dohi T, Hasizume M, Konishi K, Hata N. Ultrasound guided motion adaptive instrument for percutaneous needle insertion therapy. In: 6th International conference on biomedical engineering and rehabilitation engineering. China: Guilin; 2002. p. 225–7.
28. Solomon SB, Patriciu A, Bohlman ME, et al. Robotically driven interventions: a method of using CT fluoroscopy without radiation exposure to the physician. *Radiology.* 2002;225:277–82.
29. Jacobi V, Thalhammer A, Kirchner J. Value of a laser guidance system for CT interventions: a phantom study. *Eur Radiol.* 1999;9:137–40.
30. Lehman DS, Hruba GW, Phillips CK, McKiernan JM, Benson MC, Landman J. First prize (tie): laparoscopic renal cryoablation: efficacy and complications for larger renal masses. *J Endourol.* 2008;22(6):1123–7.
31. Farrell MA, Charboneau JW, Callstrom MR, Reading CC, Engen DE, Blute ML. Paranephric water instillation: a technique to prevent bowel injury during percutaneous renal radiofrequency ablation. *AJR Am J Roentgenol.* 2003;181(5):1315–7.
32. Haas NB. Surveillance for renal cell cancer recurrence: which patients should undergo imaging, how often, and when? *J Clin Oncol.* 2015;33(35):4131–3.
33. Ma Y, Bedir S, Cadeddu JA, Gahan JC. Long-term outcomes in healthy adults after radiofrequency ablation of T1a renal tumours. *BJU Int.* 2014;113(1):51–5.
34. Kim SD, Yoon SG, Sung GT. Radiofrequency ablation of renal tumours: four-year follow-up results in 47 patients. *Korean J Radiol.* 2012;13(5):625–33.
35. Tracy CR, Raman JD, Donnally C, Trimmer CK, Cadeddu JA. Durable oncologic outcomes after radiofrequency ablation: experience from treating 243 small renal masses over 7.5 years. *Cancer.* 2010;116(13):3135–42.
36. Balageas P, Cornelis F, Le Bras Y, et al. Ten-year experience of percutaneous image-guided radiofrequency ablation of malignant renal tumours in high-risk patients. *Eur Radiol.* 2013;23(7):1925–32.
37. Ramirez D, Ma YB, Bedir S, Antonelli JA, Cadeddu JA, Gahan JC. Laparoscopic radiofrequency ablation of small renal tumours: long-term oncologic outcomes. *J Endourol.* 2014;28(3):330–4.